American Meteorological Society
14th Conference on Interactions of the Sea and Atmosphere
30 January – 2 February 2006, Atlanta , Georgia

8.2

USE OF REAL-TIME HIGH FREQUENCY RADAR OBSERVATIONS TO ESTIMATE WINDS THAT CAN BE USED AS PART OF ON-LINE OBJECTIVE ANALYSES IN CALIFORNIA COASTAL REGIONS

Jessica Drake and John F. Vesecky
Electrical Engineering Dept., University of California at Santa Cruz, 1156 High St., Santa Cruz CA 95064
831-459-4099, fax 831-459-4829, vesecky@soe.ucsc.edu
Francis L. Ludwig
Environmental Fluid Mechanics Laboratory,
Stanford University, Stanford, CA 94305-4020
650-725-5948, fax 650-725-9720, fludwig@stanford.edu
Douglas Sinton
Meteorology Dept., San Jose State University, One Washington Square, San Jose, CA 95192-0104
408-924-5181, fax 408-924-5191, sinton@met.sjsu.edu
Jeffrey D. Paduan
Dept. of Oceanography, Naval Postgraduate School, 833 Dyer Rd., Monterey, CA 93943
831-656-3350, fax 831-656-2712, paduan@nps.edu

I. Introduction

Winds in coastal areas are both important and difficult to measure. In the San Francisco and Monterey Bay areas, several systems offer data via real-time web access. These include high frequency (HF, decameter wavelength) ground-wave radars at multiple frequencies and on shore and offshore (buoy) anemometers. This paper contains a brief review of our empirical technique for measuring ocean winds with surface-wave HF radar, and reports how we integrate those winds into a system for objective analysis of routine meteorological information and finally produce a wind field map over the San Francisco and Monterey Bay areas – land and sea.

HF radar has established itself as a useful tool for observing near surface currents in the coastal ocean. Radar observations of ocean currents are not directly related to winds, but the shear in surface currents results from wind stress at the surface. Current shear can be estimated from radar measurements at multiple frequencies (Meadows, 2002), making it reasonable to consider estimating winds from radar data. The M0 and M1 buoys (see Fig, 1) can provide independent data for building and testing empirical wind estimation methods, The buoys are maintained by the Monterey Bay Aquarium Research Institute. (MBARI)

Onshore anemometer data obtained from many sources around San Francisco Bay are archived by the U. S. Geological Survey (USGS) and San Jose State University (SJSU). These archives also include several sites around Monterey Bay that can be used with an objective analysis computer program to estimate winds over both the San Francisco and Monterey Bays. The inclusion of wind estimates from radar observations adds important information for the analyses (Vesecky et al., 2005). The objective analysis of all these merged data is the final product that is published in real-time via the WWW.

Corresponding Author Address: Jessica A. Drake, Electrical Engineering Dept., University of California at Santa Cruz, 1156 High St., Santa Cruz CA 95064, Jessica.Drake@gmail.com

2. Methods

2.1 Measurement of ocean surface currents and winds with high-frequency radar

High frequency, ground-wave radar is useful for observing near surface currents in the coastal ocean (e.g. Barrick et al. 1985). The radars detect currents because constructive interference gives returns almost exclusively from a single (Bragg resonant) ocean wavelength equal to half the radar wavelength. Oversimplifying, the radar deduces radial current components from the difference between the radar return's Doppler shift and the expected Doppler shift due to the theoretical gravity wave speed (in the absence of surface current) for the observed ocean wavelength. *Effective depth* of the current measurement depends on the radar wavelength, with longer waves *feeling* the current to greater depths. Theoretical (Stewart and Joy, 1974) and empirical (Teague et al. 2001) relationships have been developed between effective current measurement depth and wavelength.

Multiple radars observing the same area of the ocean, with some straightforward trigonometry, provide estimates of the two dimensional current

motion. In this method we typically use data from multi-frequency coastal radars (MCR's), measuring currents at depths to a few meters below the surface. MCR systems are research tools built by a consortium: University of Michigan, Veridian ERIM International, Stanford University and University of California at Santa Cruz. At present we also use data from one MCR and four Codar OS SeaSondes. Frequencies and effective depths are shown in Table 1.

Radar echoes from waves moving toward the radar differ from those moving away, causing asymmetry in radar reflectivity that can be used to determine wind direction (but not speed). Among others, Long and Trizna (1973) and Georges et al. (1993) developed methods for using the Bragg return signal strength difference between the positive Doppler (approaching wave) echo and the negative Doppler (receding wave) signal (ΔS in dB) to estimate wind direction relative to the radar line of sight (θ, degrees). We use the relationship developed by Georges et al. (1993) :

$$\left.\begin{array}{c}\theta = 0^\circ \\ \theta = \pm 180\left(\dfrac{24 + \Delta S}{48}\right) \\ \theta = 180^\circ\end{array}\right\} \quad for \quad \left\{\begin{array}{l}\Delta S \le -24 \\ -24 < \Delta S < 24 \\ \Delta S \ge 24\end{array}\right. \qquad (1)$$

Winds toward (θ=180°) or away from (θ=0°) the radar have no ambiguity, but Equation 1 gives two possibilities for all other directions, e.g. when ΔS=0 dB, wind direction will be at right angles to the look direction, either from the right or left.

TABLE 1: Operating frequency and effective depth of measured ocean currents of radars operating in the Monterey Bay, used for this study.

Radar type	Location	Frequency (MHz)	Effective Depth (m)
MCR	Santa Cruz 1	4.80	2.5
	Santa Cruz 2	6.80	1.8
	Santa Cruz 3	13.55	0.9
	Santa Cruz 4	21.77	0.6
CODAR	Moss Landing	22.8	0.6
	Naval Post Grad	13.47	0.9
	Pt. Pinos	13.40	0.9
	Santa Cruz	12.15	0.9

Steady-state conditions (admittedly infrequent) produce wind profiles and ocean current profiles that are related to the friction velocity at the surface. According to Meadows (2002), the air friction velocity (u_{*a}) is related to the friction velocity in water (u_{*w}) through the ratio of air/water densities (ρ_a/ρ_w). The equation is:

$$\frac{u_{*w}}{u_{*a}} = \left(\frac{\rho_a}{\rho_w}\right)^{0.5} \approx \left(\frac{1.1}{1025}\right)^{0.5} \approx 0.033 \qquad (2)$$

Seawater density (ρ_w=1025 kg m^{-3}) is used to get the constants in Equation 2, but the result is essentially the same for fresh water. It should be possible to determine u_{*w} from the MCR current profile, then determine u_{*a} from Equation 2. Hasse and Weber (1985) show how wind speed and u_{*a}. are related. They use a drag coefficient of 1.3×10^{-3} and showed that the wind speed at 10 m, $u_{10}\approx 28u_{*a}$. Substituting in Equation 2, then gives

$$u_{10} \approx 840 u_{*w} \quad . \qquad (3)$$

The preceding discussion suggests that there is enough information to estimate wind speed and direction directly from MCR observations, but it has been difficult. One reason for the difficulties may be large number of confounding variables. We sought a statistical approach that uses MCR information in a way that might filter out noise and incorporate variables whose relationship is not fully understood. The approach adopted below uses the MCR Bragg line ratios and MCR and SeaSonde radial and vector currents as a training data set for the method of Partial Least Squares (PLS, StatSoft 2004).

Partial Least Squares was developed in the 1960's by economist Herman Wold for modeling poorly understood relationships with collinear input variables. To illustrate how PLS works we will first look at comparable methods. (StatSoft, 2004; Tobias, 1995)

At the center of any linear regression is the equation:

$$y = b_0 + x_1 b_1 + x_2 b_2 + \ldots + x_p b_p + \varepsilon \qquad (4)$$

where ε is residual error; x is the input data, y is the prediction and b are coefficients. In matrix form this becomes

$$\mathbf{Y = XB + E} \qquad (5)$$

where ***X*** is the input data having n cases by p variables, ***Y*** is the prediction data having n by m responses, ***B*** is p by m and **E** is an error matrix.

Various techniques for solving for ***B*** include Multiple Linear Regression (MLR), Principal Components Regression (PCR), and Maximum Redundancy Analysis (MRA). MLR uses a least squares approach to solve for ***B***, which requires matrix inversion. MLR requires relationships between predicted and input variables to be clearly defined, no co-linearity in the input variables and the number of input variables must not exceed the number of samples. PCR first breaks down the data into ***X***-scores using a decomposition of ***X***'***X***, where the prime denotes the transpose. The ***X***-scores capture the maximum variability in the input data and are then regressed (using least squares) against the prediction variables to generate ***B***. However, PCR focuses on the largest variability of the input data, which may not be correlated to the prediction variables. MRA uses

a decomposition of ***Y***'***Y*** to calculate ***Y***-scores. This captures the variability of the prediction data in the regression, but still ignores the correlations between the ***X*** and ***Y*** data, and tends not to be stable. PLS calculates scores using a decomposition of the matrix ***Y***'***XX***'***Y***. Skipping how, the decomposition calculates the p by c matrix ***W*** such that ***T*** = ***XW***, and ***T*** has the maximum correlation with the prediction data. This means that ***W*** captures the space that best relates to the prediction variables. With the hard part done, least squares is used to calculate ***Q*** from ***Y*** = ***TQ*** + ***E***, and the matrix of coefficients ***B*** is simply ***WQ***.

PLS is considered linear because of the linear regression between ***Y*** and ***T***. However, if analysis shows that while ***Y*** and ***T*** are highly correlated they do not have a linear relationship, (i.e. $y_{ij} = t_{ij}^2 + e$), the appropriate relationship can be inserted at that step. Because the mathematical relation is on ***T*** calculated from ***T*** = ***XW***, the model can no longer be simplified to ***B*** = ***WQ***. Rather, ***W*** and ***Q*** must be retained in order to generate future predictions.

In our case, the input data matrix X is built from radar data, calculated at the M0 and M1 buoy locations (See Figure 1 below), and the response matrix Y is derived from winds measured at the buoys. Each radar measures radial current vectors; if the radial vectors for the different radars are sufficiently different, and the radar frequencies are similar, then straightforward trigonometry can be used to calculate total current vectors.

The MCR also generates Bragg Line ratios, giving a choice of two possible wind directions for each frequency (see Eq. 1). The problem is to determine which of the two directions is most likely. We assume that the horizontal wind shear is not great, so that wind directions derived from nearby locations should be similar. Using this assumption, directions at nearby locations are compared by adding and subtracting the Bragg Line wind direction to the look angle; those pairs that produce the smallest spatial changes in wind direction are chosen, and used as inputs to the PLS methodology, which determines their proper weighting. The format of the X matrix is based on what data are available to allow flexibility. A separate X matrix is required at every point for which we would want a wind estimate. Thus, each combination of data requires it's own PLS model to generate a wind estimate.

As noted, the PLS algorithm was applied to a subset of data, called the 'training' set. Typically, we used 1/6 to 1/3 of the available data taken over an 8–month period for training. The resulting PLS prediction model was applied to the remaining data to validate the model.

The many factors that go into generating a calibration model break down into three steps: 1) choosing a training sample set; 2) deciding which, if any, non-linear mathematical treatments should be done in the PLS; and 3) determining which, if any, non-linear mathematical treatments should be applied to portions of the radar data. Of these, the first, choosing a training set that totally encompasses the data space and has an even distribution of both signal and noise, is generally the most important.

A computer script has been written to generate of few training sets and test the many possible combinations. To rank the models, the algorithm calculates the bias and standard error of prediction (SEP) for four groups, high and low +/- wind vectors. Each section is weighted by performance in such a way that if the model has large errors in one section those errors carry the most weight. A model that has near perfect estimation in 3 sections but fails the 4th (i.e. cannot predict high positive wind vectors) will rank lower than a model that has moderate but consistent performance across the whole range of data. The top 20 or so are then evaluated by eye to select the most robust model.

2.2 Objective analysis with the Winds on Critical Streamline Surfaces (WOCSS) methodology

The Winds on Critical Streamline Surfaces (WOCSS) methodology (Ludwig et al. 1991) provides objective analyses of wind observations that account for the fact that stable layers in the atmosphere suppress vertical motions and force air flow around hills and ridges, rather than over them. Briefly, the WOCSS code defines surfaces on which flow should take place, given that there is a maximum height to which the kinetic energy of the wind can lift a parcel of air in a stably stratified atmosphere. The maximum height is based on the critical dividing streamline concept, and assumes that air parcel vertical displacement in complex terrain balances the original kinetic energy of the flow at low altitudes, and the energy required to change altitude in the presence of a buoyant restoring force (see e.g. Sheppard 1956; Hunt and Snyder 1980; McNider et al. 1984). This energy constraint leads to a relationship among potential temperature lapse rate ($d\theta/dz$), the maximum height to which the air can rise (Z_{max}), and the low-altitude wind speed V_0 at the lowest height (z_0) for a particular low surface:

$$Z_{\max} - z_0 = V_0\left(\frac{g}{\overline{T}}\frac{d\theta}{dz}\right) \quad . \tag{6}$$

$\overline{T}$ is the mean temperature between z_0 and Z_{max}, and *g* is the gravitational constant.

The low altitude wind speed V_0 is defined from winds first interpolated to terrain-following surfaces. Equation 6 determines the maximum height for each of a number of flow-following surfaces, which may intersect the terrain when the atmosphere is stable. A second interpolation defines winds on the new surfaces. Then, these "first guess" winds are iteratively adjusted to reduce two-dimensional divergence on the flow surfaces. Winds are set to zero where the flow surfaces intersect the terrain so the iterative adjustments force flow around the terrain obstacles. The code also includes provisions so that the presence of a stable layer at one altitude will influence flow at levels above and below that layer. The method performs well when there is adequate

input data (Bridger et al. 1994; Ludwig and Sinton 2000).

3. Results

To generate wind estimates from radar data, the radar data from each site is collected. For each point over the bay, the data is processed, and if enough signal is available, compiled into a matrix. The appropriate PLS model for that matrix format is then applied to generate a wind estimate.

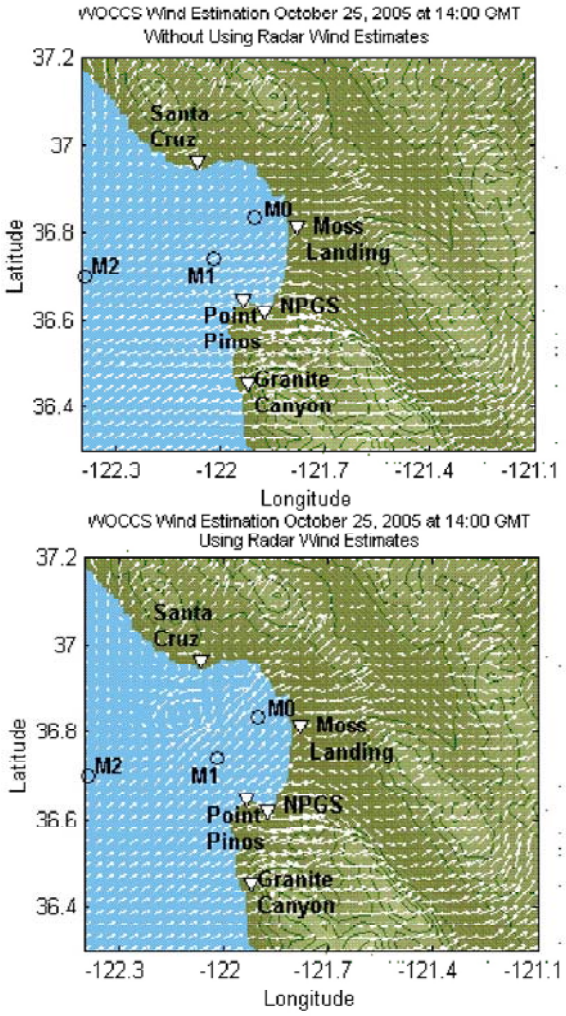

Figure 1 Radar and buoy locations, and wind fields without (upper panel) and with (lower) use of radar wind estimates over Monterey Bay.

The radar wind estimates are then merged with the most recent Oakland and Vandenberg Air Force Base soundings anemometer readings around the San Francisco and Monterey Bay areas to provide the inputs for the WOCSS analysis which generates wind estimate that cover an area approximately 222 km (N-S) by 177 km (E-W). Figure 1 shows a subsection of the larger grid. The full area of coverage is shown in Figure 2. Buoy wind measurements from the M0, M1 and M2 moorings are not used at present since we do not currently have access to them without a time delay that precludes achieving our goal of providing real time wind fields. We anticipate that the latency of the buoy wind measurements can be reduced and that they soon can be used in this objective analysis.

The winds are plotted with 1-km spacing in Figure 1, and 4-km spacing in Figure 2, although the calculations were done on a 1-km grid in both cases. Unlike anemometer measurements that represent winds at a point, the winds based on HF radar measurements roughly represent averages over areas three to five km across. The merging of the two kinds of data does not present a problem, because spatial averaging is already inherent in the interpolation used to get first guess fields for the WOCSS analysis (Ludwig et al., 2006).

Earlier studies (Drake et al. 2004) showed that the addition of radar information changed the average winds by as much as 15° in direction and 3 m s^{-1} in speed. Comparison of the two panels in Figure 1 shows that the effects can be much larger for individual cases. The radar has detected a small eddy just south of Santa Cruz. Archer et al. (2005) have deduced the presence of such eddies from the few buoy observations, onshore measurements and satellite imagery, but the availability of the radar data may make it easier to identify these circulations in the future and better understand the mechanisms that cause them.

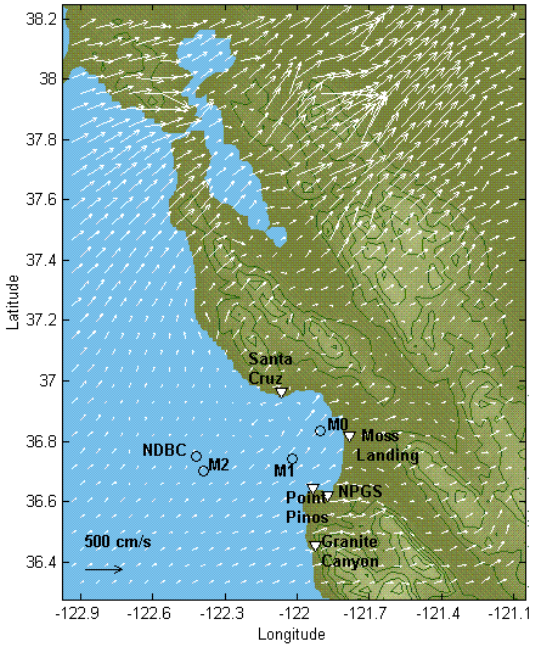

Figure 2 Complete area of coverage for the analyses.

4. Summary and Conclusions

HF radar observations of the ocean surface in coastal areas already provide very valuable information about the ocean currents. The studies described here have shown that these same radar observations also contain very valuable information about the winds over the water. However, that information cannot be easily extracted by

straightforward methods. Nevertheless, the PLS approaches discussed here have proven effective in estimating winds at the buoy locations where the results can be verified.

Once the winds over water have been determined from the radar observations, it is quite easy to combine them with conventional anemometer measurements to provide a more complete set of inputs for the WOCSS objective analysis methods. The preliminary results given here demonstrate the value of the additional radar information. The example in Figure 1 showed that without the radar data, the analyses did not detect the presence of the smaller scale eddy circulation. Such circulations are believed to be present quite frequently over Monterey Bay, and they often go undetected.

In summary, multifrequency coastal HF radar measurements of the wind, together with buoy and land based anemometers can be used with the WOCSS objective analysis to produce wind fields over the coastal land and ocean with good time and space resolution. Coastal HF radars help make up for the sparse deployment of coastal buoys and improve wind field estimates over the ocean.

HF radar systems will be installed along the entire California coast over the next three years and they are being deployed with increasing density along other parts of the US coastline. Although most of these units are not multiple frequency, as required for wind estimation, they could be modified at a relatively small (but not insignificant) cost. The availability of real-time wind fields produced using the methods demonstrated here would find extensive application in coastal science and engineering that should offset any additional cost. These newly available wind estimates would improve environmental monitoring and prediction, and aid in brush and forest fire control, air and sea rescue and coastal recreation activities, such as fishing, boating, sailing, wave and wind surfing,

Acknowledgements. This work was supported through the School of Engineering, University of California at Santa Cruz by the Office of Naval Research (Charles Luther, Scientific Officer) under ONR Grant N00014-97-1-0375. We are grateful to Francisco Chavez and the Monterey Bay Aquarium Research Institute for providing the wind data from the M0 and M1 buoy, and to Prof. Douglas Sinton of San Jose State University and Dr. Ralph Cheng of the U. S. Geological Survey for making available the wind data archived from the USGS web site.

References

Archer, C. L., M. Z. Jacobson and F. L. Ludwig, 2005: The Santa Cruz Eddy. Part I: Observations and Statistics, *Mon. Wea.. Rev.* **133**,, 767–782.

Barrick, D. E., B. J. Lipa, and R. D. Crissman, 1985: Mapping surface currents with CODAR, *Sea Tech.*, **26**, 43-48.

Bridger, A. F. C., A. J. Becker, F. L. Ludwig and R. M. Endlich, 1994: Evaluation of the WOCSS Wind Analysis Scheme for the San Francisco Bay Area, *J. Appl. Meteorol.,* **33***,* 1210-1218.

Drake, J., F. L. Ludwig and J. Vesecky, 2004: Using High Frequency radar observations of the ocean surface and objective analyses of onshore observations to estimate winds over Monterey Bay, California, Presented at 13th Conf. on Interactions of the Sea and Atmosphere. Paper 1.6, Aug. 2004, Portland, ME, Amer. Meteorol. Soc., Boston MA,.

Georges, T. M. J. A. Harlan, L. R. Meyer, and R. G. Peer, 1993: Tracking Hurricane Claudette with the U.S. Air Force Over-the-Horizon Radar, J. Atmos and Oceanic Tech., 10, pp. 441-451.

Hasse, L. and H. Weber, 1985: On the conversion of Pasquill categories for use over sea, *Bound. Lay. Meteor.*, **31**, 177-185.

Hunt, J. C., and W. H. Snyder, 1980: Experiments on Stably and Neutrally Stratified Flow Over a Three-dimensional hill. *J. Fluid Mech*., **96**, 671-704.

Long, A. E. and D. B. Trizna, 1973: Mapping of North Atlantic Winds by HF Radar Sea Backscatter Interpretation", *IEEE J. Antennas and Propagat.* , **AP-21**, 680-685.

Ludwig, F. L., J. M. Livingston, and R. M. Endlich, 1991: Use of mass conservation and dividing streamline concepts for efficient objective analysis of winds in complex terrain, *J. Appl. Meteor.,* **30**, 1490-1499.

Ludwig, F. L., D. K. Miller, and S. G. Gallaher, 2006: Evaluating a hybrid prognostic/ diagnostic model that improves wind forecast resolution in complex coastal topography. *J. Appl. Meteorol, in press*.

Ludwig, F. L. and D. Sinton, 2000; Evaluating an objective wind analysis technique with a long record of routinely collected data, *J. Appl. Meteorol.,* **39,** 335-348.

Meadows, L. A., 2002: *High frequency radar measurements of friction velocity in the marine boundary layer*, PhD dissertation, U. of Mich., Ann Arbor, MI, 125 pp.

McNider, R. T., K. E. Johnson and R. W. Arritt, 1984: Transferability of Critical Dividing Streamline Models to Larger Scale Terrain. Preprints *4th Joint Conf. on Applic.s of Air Poll. Meteorol.,*, Amer. Meteor. Soc., Boston, J25-J27.

Sheppard, P. A., 1956: Air flow over mountains. *Quart. J. Roy. Meteor. Soc*., **82**, 528-529.

StatSoft, 2004: *Electronic Statistics Textbook*, StatSoft, Inc., Tulsa, OK, available at http://www. statsoft.com/textbook/stathome.html.

Stewart, R. H. and J. J. Joy, HF radio measurements of ocean surface currents, *Deep Sea Res., 21*, 1039-1049.

Teague, C. C. J. F. Vesecky and Z. Hallock*.,* 2001: A comparison of multifrequency HF radar and ADCP measurements of near surface currents during COPE-3, *J. Oceanic Engin., 26*, 3, 399-405.

Tobias, R. D. 1995: An introduction to partial least squares regression, *Proc. 20th SAS Users Group Internat.***,** SAS Institute Inc., Cary, NC., 8 pp.

Vesecky, J. F., J. A. Drake, K. E. Laws, F. L. Ludwig, C. C. Teague, J. D. Paduan & L. A. Meadows, 2005: Using multifrequency HF radar to measure ocean wind fields, Proc. Intl. Geosci. & Remote Sens. Sym., IEEE Press, Piscataway NJ.